AGN SURVEYS
ASP Conference Series, Vol. 284, 2002
R.F. Green, E.Ye. Khachikian, D.B. Sanders

AGN Populations from Optical Identification of *ASCA* Surveys

Masayuki Akiyama

Subaru Telescope, National Astronomical Observatory of Japan, Hilo, HI, 96720

Yoshihiro Ueda

ISAS, Sagamihara, Kanagawa, 229-8510, Japan

Kouji Ohta

Department of Astronomy, Kyoto University, Kyoto, 606-8502, Japan

Abstract. To understand luminous AGNs in the $z < 1$ universe, the *ASCA* AGN samples are the best at present. Combining the identified sample of AGNs from the *ASCA* Large Sky Survey and Medium Sensitivity Survey, the sample of hard X-ray selected AGNs has been expanded up to 108 AGNs above a flux limit of 10^{-13} erg s^{-1} cm^{-2} in the 2–10 keV hard X-ray band. We discuss the fraction of absorbed AGNs in the hard X-ray selected AGN sample, and the nature of absorbed luminous AGNs.

1. Introduction : Importance of a Bright Hard X-ray AGN sample

The fraction of absorbed AGNs, especially luminous absorbed AGNs, is a big issue in understanding the true number density of active nuclei in the universe. Recently many candidates for absorbed luminous AGNs have been found in AGN surveys in radio, X-ray, and near-infrared wavelengths (e.g., Webster et al. 1995). The discoveries imply that we have been missing a significant fraction of nuclei with high activity in traditional optical/UV-selection of AGNs due to absorption toward the nucleus. However, the fraction of absorbed AGN in the entire AGN population is not clear. Radio-selected samples are affected by red AGNs with red synchrotron components (Francis et al. 2001), soft X-ray selection is biased against heavily absorbed AGNs (Kim & Elvis 1999), and 2MASS-selected red AGNs are limited to the low-redshift universe (Cutri et al. in this volume).

In order to construct a complete sample of AGNs less biased against absorption toward the nucleus, we conducted optical follow-up observations for the *ASCA* Large Sky Survey (hereafter ALSS; Ueda et al. 1999) and the *ASCA* Medium Sensitivity Survey (hereafter AMSS; Ueda et al. 2001) in the hard X-ray band. Hard X-ray emission can penetrate the obscuring matter of absorbed AGNs and is very suitable to search for absorbed AGNs. Using 2–10 keV hard X-ray emission, we can detect AGNs with X-ray absorption up to hydrogen col-

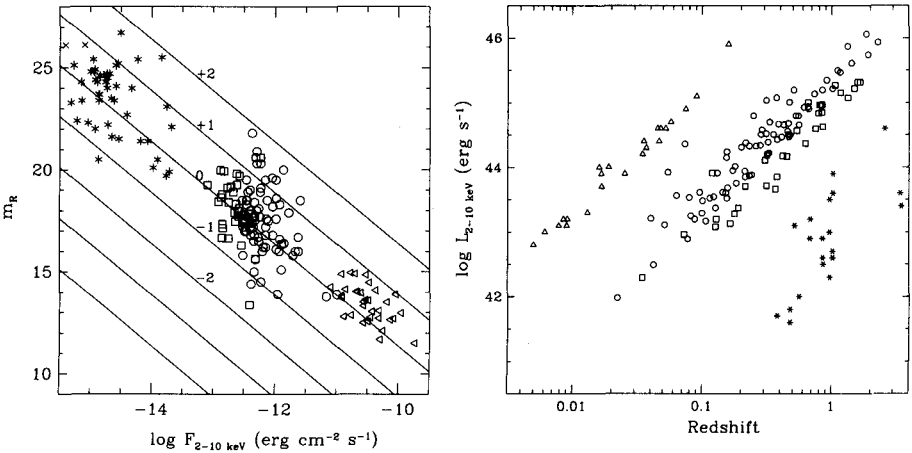

Figure 1. Left) R-band magnitudes of optical counterparts of ALSS (square) and AMSSn (circle) AGNs are plotted as a function of 2–10 keV hard X-ray flux. Dashed lines represent the X-ray to optical flux ratio of $\log f_X/f_V = +2,+1,0,-1$,and -2 from top to bottom. Triangles and asterisks indicate samples from *HEAO1* A2 (Piccinotti et al. 1982) and the *Chandra* survey in the HDF-N (Hornschemeier et al. 2001) Right) Hard X-ray luminosities of hard X-ray selected AGNs plotted as a function of redshift. Same symbols as in the left panel.

umn density of $10^{22\sim23}$ cm^{-2}, which corresponds to A_V of $20 \sim 50$ with the Galactic conversion factor, without bias. The ALSS is a survey in a continuous field of 5.4 square degrees near the North Galactic Pole. We selected 34 X-ray sources detected with SIS 2–7 keV significance greater than 3.5σ. The sources are identified with 30 AGNs, 2 clusters of galaxies and 1 galactic star (Akiyama et al. 2000). One X-ray source with a hard spectrum is still unidentified, and a *Chandra* follow-up observation is planned in Cycle 3. The AMSS is a serendipitous source survey based on *ASCA* pointed observations conducted in high galactic latitude regions ($|b| > 20°$). We conducted optical follow-up observations for 86 X-ray sources detected with GIS 2–10 keV significance greater than 5.6σ in the northern sky (declination above 20°; we call it the AMSSn sample). All of the X-ray sources are identified with 78 AGNs, 7 clusters of galaxies, and 1 galactic star (Akiyama et al. in preparation). In total, we constructed a sample of 108 hard X-ray selected AGNs with a flux limit of *ASCA*, $\sim 10^{-13}$ erg s^{-1} cm^{-2} in the 2–10 keV band. In Figure 1, we plotted the hard X-ray flux vs. optical magnitude (left) and the redshift vs. luminosity distribution (right) diagrams of ALSS and AMSSn AGNs. The *ASCA* samples are two orders of magnitude brighter and more luminous than the sample of deep *Chandra* and *XMM-Newton* surveys, and consists of luminous AGNs, i.e., QSOs, in the universe below redshift 1. The high completeness of the *ASCA* samples makes it possible to discuss the fraction of absorbed AGNs definitively.

https://doi.org/10.1017/S0252921100030761 Published online by Cambridge University Press

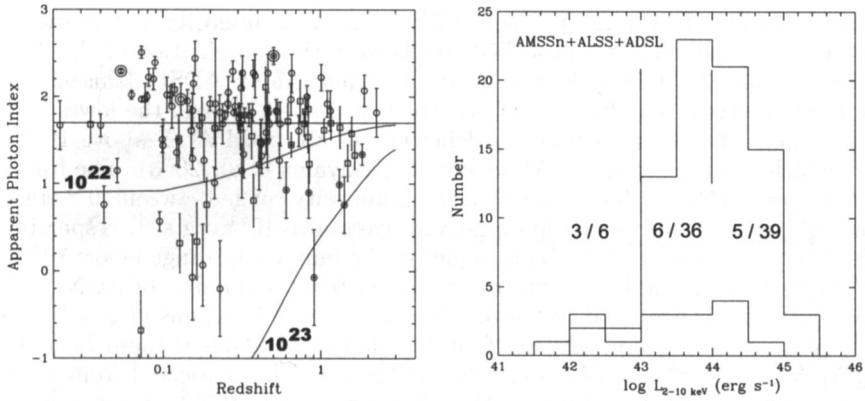

Figure 2. (Left) Apparent photon indices of ALSS (squares) and AMSSn (circles) AGNs in the 0.7–10 keV hard X-ray band are plotted as a function of redshift. BL Lac objects are marked with large circles. The solid lines show the apparent photon index of a power-law continuum with intrinsic photon index of 1.7 absorbed by hydrogen column density of 10^{22} cm^{-2} (top) and 10^{23} cm^{-2} (bottom) at each redshift. AGNs with a faint optical counterpart ($\log f_X/f_V$ larger than 1) are marked with dots. (Right) Luminosity distributions of all (thin) and significantly absorbed (thick) AGNs below a redshift of 0.6 from a combination of the AGN samples of the ALSS, AMSSn, and ADSL.

2. Fraction of Heavily Absorbed AGNs

Using the hardness of the X-ray spectrum of each source, we can estimate the X-ray absorption to the nucleus in each object. The 0.7–10 keV apparent photon index distributions of ALSS and AMSSn AGNs are plotted as a function of redshift in the left panel of Figure 2. The upper and lower solid lines in the figure correspond to the apparent photon index of an object with intrinsic photon index of 1.7 and X-ray absorption with hydrogen column density of $\log N_{\rm H} = 22(\rm cm^{-2})$ and $\log N_{\rm H} = 23(\rm cm^{-2})$ at each redshift, respectively. The X-ray sources with apparent photon index smaller than 1 can be regarded as significantly harder than canonical power-law spectra of broad-line AGNs (with photon index of 1.7). They correspond to intermediate redshift AGNs with X-ray absorption of $\log N_{\rm H} = 22 - 23(\rm cm^{-2})$ and high-redshift AGNs with absorption of $\log N_{\rm H} > 23(\rm cm^{-2})$. At high-redshift ($z \sim 1$), the apparent photon indices of highly absorbed objects become close to that of an object without absorption, because we observe very high energy photons from the source-frame, which are less affected by absorption than low-energy photons.

Based on the estimated amount of absorption to the nucleus, we examine the fraction of absorbed AGNs in the hard X-ray selected AGNs. For simplicity, we limit the sample to redshifts less than 0.6, and regard AGNs with $\log N_{\rm H} > 22(\rm cm^{-2})$ as significantly absorbed AGNs. It should be noted that at high redshifts ($z > 0.6$), AGNs with hydrogen column densities of $\log N_{\rm H} = 10^{22-23}$ (cm^{-2}) cannot be regarded as significantly absorbed in the

https://doi.org/10.1017/S0252921100030761 Published online by Cambridge University Press

current sample. In the right panel of Figure 2, the luminosity distributions of all AGNs and significantly absorbed AGNs from the combination of the ALSS, AMSSn, and *ASCA* Deep Survey in the Lockman Hole (ADSL; Ishisaki et al. 2001) are plotted. The fraction of absorbed AGNs is higher in the lowest luminosity range, but there is no clear deficiency of absorbed AGN above 10^{44} erg s^{-1}, which is observed in the ALSS sample (Akiyama et al. 2000). The fraction of absorbed AGN is 6/36 and 5/39 in the luminosity range between 10^{43} erg s^{-1} and 10^{44} erg s^{-1} and in the luminosity range above 10^{44} erg s^{-1}, respectively. The fraction of absorbed AGNs is higher in the luminosity range below 10^{43} erg s^{-1} (3/6) than in the luminosity range above, but the number of AGNs in the low luminosity range is fairly limited. The fraction of luminous ($L_X > 10^{44}$ erg s^{-1}) AGNs with $\log N_H > 22(cm^{-2})$ in the sample of AGNs without bias up to $\log N_H = 23(cm^{-2})$ ($\sim$15%) is clearly smaller than that expected from models of the cosmic X-ray background (45%; Comastri et al. 1995) or that observed in local low-luminosity Seyfert galaxies (40%; Risaliti et al. 1999).

3. Case Studies of Absorbed QSOs

The fraction of absorbed QSOs is not as large as expected, but we detected several candidates for absorbed QSOs in the *ASCA* surveys. Their counterparts are relatively faint and have larger X-ray to optical flux ratios than normal AGNs (see dotted objects in the left panel of Figure 2). Most of the high-redshift AGNs with hard X-ray spectra have large X-ray to optical flux ratios. The X-ray to optical flux ratio is similar to those of the optically-faint hard X-ray source population found in deep *Chandra* surveys (see left panel of Figure 1; e.g., Alexander et al. 2001), and the *ASCA* optically-faint AGNs can be low-redshift and/or high-luminosity cousins of the *Chandra* population.

Although the measured amount of X-ray absorption is large, most of the luminous absorbed QSOs show broad MgII 2800Å or Hα 6563Å emission lines. The origin of the discrepancy can be 1) broad MgII 2800Å from scattered nuclear light or 2) a discrepancy between the amount of X-ray photoelectric absorption and optical dust reddening. We show two examples of absorbed QSOs that fall in each category.

3.1. An absorbed QSO at $z = 0.65$ with a strong broad MgII 2800Å emission line

AX J131831+3341 is an absorbed radio-quiet QSO at a redshift of 0.65 found in the ALSS (Akiyama et al. 2000). Its X-ray luminosity is estimated to be $\sim 10^{45}$ erg s^{-1}, which corresponds to the luminosities of QSOs. The observed X-ray spectrum of the object in the 0.7–10 keV band is described by intrinsic absorption with a hydrogen column density of $N_H = 6.0^{+4.4}_{-4.2} \times 10^{21}$ cm^{-2} and an intrinsic photon index of 1.7. The hydrogen column density corresponds to the lower edge of the column density distribution of Seyfert 1.8-1.9 galaxies.

The optical spectrum of the object shows strong emission lines, such as broad MgII 2800Å, narrow [O II] 3727Å, and narrow [O III] 5007Å, but no broad Hβ emission line (see right panel of Figure 3). Its small Hβ-to-[O III] 5007Å equivalent width ratio is comparable to those of Seyfert 1.8-2 galaxies. Optical and near-infrared images show nuclear and extended components (see

https://doi.org/10.1017/S0252921100030761 Published online by Cambridge University Press

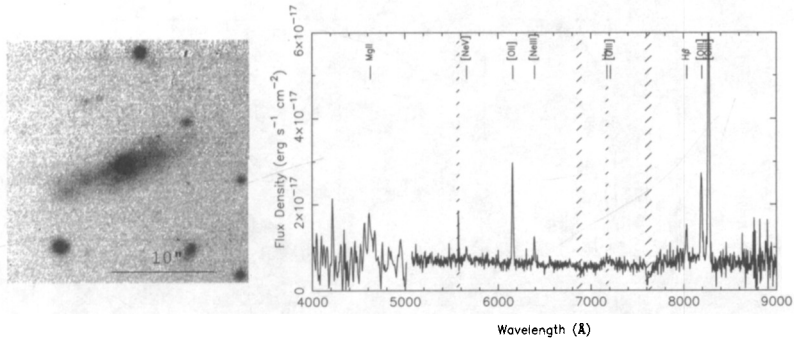

Figure 3. (Left) Optical R-band image of AX J131831+3341. (Right) Optical spectrum of AX J131831+3341. An 1800s FOCAS/Subaru spectrum above 5000Å with a 3600s MOSCA/Calar Alto 3.5m spectrum around MgII 2800Å emission.

left panel of Figure 3). Because the nuclear component has a very red $I - K$ color but blue $V - R$ and $R - I$ colors, the nucleus is thought to be absorbed with $A_V \sim 3$ and to emerge only in the K-band (Akiyama and Ohta 2001). The amount of absorption is consistent with the amount of X-ray absorption. The optical blue continuum and broad MgII 2800Å emission line can originate from scattered nuclear light (Akiyama et al. 2001).

3.2. A candidate for a type-2 QSO with large X-ray absorption and a strong broad-Hα emission line

AX J08494+4454 is a candidate for a type-2 QSO at $z = 0.9$ found in the course of optical identification of the *ASCA* deep survey in the Lynx field (Ohta et al. 1996). Recently, a deep *Chandra* hard X-ray spectrum and an IRCS/Subaru J-band spectrum of the object have been obtained (Akiyama et al. 2002). The 0.5–10 keV 150ks *Chandra* spectrum of AX J08494+4454 is hard, and is explained well with a power-law continuum absorbed by a hydrogen column density of $(2.3 \pm 1.1) \times 10^{23}$ cm^{-2}. The 2–10 keV luminosity of the object is estimated to be $7.2^{+3.6}_{-2.0} \times 10^{44}$ erg s^{-1}, after correcting for absorption, and reaches the range of hard X-ray luminosities of QSOs. The large X-ray absorption and the large intrinsic luminosity support the original identification of AX J08494+4454 as a type-2 radio-quiet QSO. Nevertheless, deep Subaru/IRCS J-band spectroscopic observation suggests the presence of a strong broad Hα emission line from AX J08494+4454 (left panel of Figure 4). The broad Hα emission line has a velocity width of 9400 ± 1000 km s^{-1}, which corresponds to a typical broad Balmer line velocity width of a luminous QSO. The existence of the strong broad Hα line means that the object is not a type-2 QSO, but a luminous cousin of a Seyfert 1.9 galaxy in the source-frame optical spectrum. The Balmer decrement of broad lines, the broad Hα emission to the hard X-ray luminosity ratio, and optical SED (right panel of Figure 4) suggest that the nucleus is affected by dust extinction with A_V of $1 - 3$ mag in optical wavelengths. The estimated amount of dust extinction is much smaller than that expected from the X-ray column density ($A_V = 130 \pm 60$ mag). The discrepancy can be explained with a smaller

https://doi.org/10.1017/S0252921100030761 Published online by Cambridge University Press

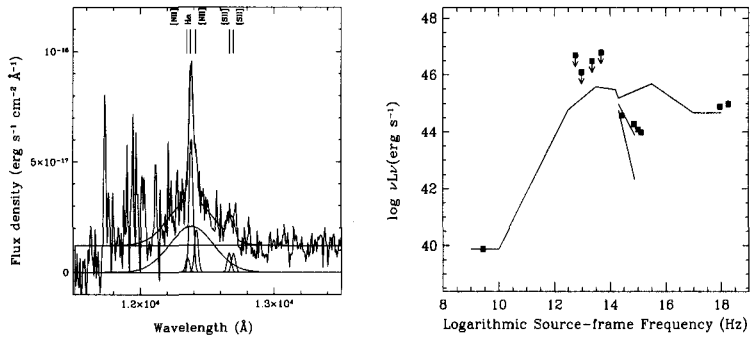

Figure 4. (Left) J-band spectrum of AX J08494+4454. The best fit models are also plotted with solid lines. (Right) Spectral energy distribution (SED) of AX J08494+4454. The solid line indicates the SED of an average radio-quiet QSO (Elvis et al. 1994) and is normalized at the data point observed at 1.4 GHz. Dashed lines represent optical SEDs with dust extinction with A_V of 1 mag (upper) and 2 mag (lower).

dust to gas mass ratio which may due to dust sublimation in the X-ray absorbing matter, the size difference between optical and X-ray emitting regions, or a different dust size distribution in AGNs (e.g., Maiolino et al. 2001).

Acknowledgments. The authors thank ALSS and AMSS members.

References

Akiyama, M., et al. 2000, ApJ, 532, 700
Akiyama, M., and Ohta, K. 2001, PASJ, 53, 63
Akiyama, M., et al. 2001, PASJ, 52, 577
Akiyama, M., Ueda, Y., and Ohta, K. 2002, ApJ, in press (astro-ph/0111037)
Alexander, D.M., et al. 2001, ApJ, in press (astro-ph/0107450)
Comastri, A., Setti, G., Zamorani, G., and Hasinger, G. 1995, A&A, 296, 1
Elvis, M., et al. 1994, ApJS, 95, 1
Francis P.J., et al. 2001, PASA, in press (astro-ph/0107235)
Hornschemeier, A., et al. 2001, ApJ, 554, 742
Ishisaki, Y., et al. 2001, PASJ, 53, 445
Kim, D., and Elvis, M. 1999, ApJ, 516, 9
Maiolino, R., Marconi, A., and Oliva, E. 2001, A&A, 365, 37
Ohta, K., et al. 1996, ApJ, 458, 57
Piccinotti, G., et al. 1982, ApJ, 253, 485
Risaliti, G., Maiolino, R., Salvati, M. 1999, ApJ, 522, 157
Ueda, Y., et al. 1999, ApJ, 518, 656
Ueda, Y., et al. 2001, ApJS, 133, 1
Webster, R., et al. 1995, Nature, 375, 469